Synthesis and Reactivity of 3-Diazo-4-oxocoumarins for Photolithographic Applications

Michael J. Leeson, Wang Yueh, Peter I. Tattersall, Adam Pawloski,
Scott M. Grayson, and C. Grant Willson*

*Departments of Chemistry and Chemical Engineering, The University of Texas at Austin,
Austin, Texas 78712-1062*

3-Diazo-4-oxocoumarins absorb in the deep ultraviolet (DUV) and upon photolysis undergo a Wolff rearrangement in aqueous environments to afford carboxylic acid photoproducts that are transparent in the DUV. Because this photochemical reaction transforms a base insoluble chromophore into a base soluble one, it may be exploited for the design of photolithographic materials. Examples of 5-, 6-, and 7-substituted 3-diazo-4-oxocoumarins have been synthesized and the reactivity of the corresponding photogenerated ketenes has been studied. For most chromophores, the rate of ketene hydrolysis was found to correlate with the calculated charge on the ketenyl carbon. 3-Diazo-4-oxocoumarins bearing electron-donating substituents in these positions demonstrate the lowest reactivity and therefore show the most promise for lithographic materials.

Introduction

Microlithographic patterning using polymeric photoresists is a key step in the manufacture of semiconductor devices.[1] Improvements in the resolution of the lithographic process leads to smaller, faster devices and hence has been a continuous goal of computer-related industries. Because the resolution of the process is inversely related to the wavelength of exposure, the exposure source for patterning has shifted from the G- and I-line (436 and 365 nm, respectively) emissions of high-pressure mercury lamps to systems using 248-nm, 193-nm, and most recently 157-nm excimer laser radiation.

Diazonaphthoquinone (DNQ)-novolac based positive tone[2] photoresists are used extensively for I-line lithography.[3] The resist formulation includes only about 10−20% of DNQ dispersed in novolac. The DNQ acts as a dissolution inhibitor which slows the dissolution rate of the novolac resin in an aqueous base by orders of magnitude, until a photochemically reaction enhances the solubility. In this system, DNQ reacts when irradiated to form a carboxylic acid, altering the solubility of the bulk material from sparingly soluble to freely soluble in aqueous base. This solubility switch can be used to transfer an image onto the polymer film. If an opaque, patterned mask is placed between a light source and the photoactive resist, the photochemical reaction will occur only in those regions that were exposed to light. This photochemical transformation significantly speeds the dissolution of the resin in exposed areas of the film relative to the rate in unexposed areas, enabling the transfer of an image from a photomask onto the polymer film via "development" with aqueous base. The residual polymer film then acts as an etch barrier, enabling the underlying surface to be patterned where the polymer layer was removed.[1,3]

The advent of 248 nm (KrF excimer laser) based exposure tools created a demand for new resists appropriate for this wavelength. DNQ-based resists do not function well at this wavelength because both the chromophore and the novolac absorb so strongly at 248 nm that light cannot penetrate thin films of these materials, leading to poorly resolved images. New 248-nm resists are all based on substituted poly-(4-hydroxystyrene) with pendant functional groups that undergo the required solubility switch when exposed to a photogenerated acid.[3] Although these chemically amplified systems based on photo acid generators are efficient and have been used widely, they have some important process sensitivities, including extreme sensitivity to airborne amine base contaminants.[4] Attempts have been made to create nonchemically amplified deep UV resist systems based on meldrum's diazo,[5,6] certain ortho-nitrobenzylesters,[7] and copolymers of methacrylic acid and methacrylate esters,[8,9] but all of these systems

(1) MacDonald, S. A.; Willson, C. G.; Frechet, J. M. J. *Acc. Chem. Res.* **1994,** *27,* 151. Thompson, L. F.; Willson, C. G.; Bowden, M. J. *Introduction to Microlithography, Second Edition*; ACS Professional Reference Book; American Chemical Society: Washington, DC, 1994.

(2) Positive tone refers to a transferal of shape of the mask onto the underlying resist film (voids in the mask reproduced as voids on the surface), and negative tone refers to a process where the reproduced image is inverted (voids in the mask are translated as polymer features on the surface, whereas the substance of the mask is translated as voids on the surface).

(3) Dammel, R. *Diazonaphthoquinone-based Resists*; SPIE-The International Society for Optical Engineering: P.O. Box 10, Bellingham, WA, 1993.

(4) MacDonald, S. A.; Hinsberg, W. D.; Wendt, H. R.; Willson, C. G.; Snyder, C. D. *Chem. Mater.* **1993,** *5,* 348.

(5) Grant, B. D.; Clecak, N. J.; Twieg, R. J.; Willson, C. G. *IEEE Trans. Electron Devices* **1981,** *28* (11*),* 1300.

(6) Willson, C. G.; Miller, R. D.; McKean, D. R.; Pederson, L. A.; Regitz, M. *SPIE Vol. 771 Advances in Resist Technology and Processing IV* **1987,** 2.

(7) Reichmanis, E.; Wilkins, C. W., Jr.; Price, D. A.; Chandross, E. A. *J. Electrochem. Soc.: Solid-State Sci. Technol.* **1983,** *130* (6), 1433.

Scheme 1. Chemical Structures of Pertinent PACs
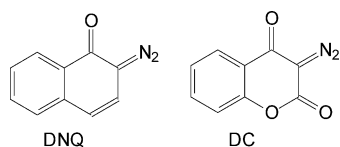
suffer from some functional deficiency. Here we describe the synthesis and evaluation of diazocoumarin based photoactive compounds (PACs) as dissolution inhibitors for 248-nm photoresist applications.

Previous work showed that 2-diazo-1,3-diones have nearly ideal spectral properties for use in the design of DUV resists.[6] It is expected that the 3-diazo-4-oxo-coumarin (DC) chromophore[10] (see Scheme 1) will make an excellent DUV photoactive compound because it incorporates this diazodione functionality and is a structural analogue of DNQ, the optimized PAC for 365-nm resists. DC, like DNQ, undergoes the Wolff Rearrangement[11] when irradiated to yield a ring-contracted ketene intermediate[12] that then reacts with adventitious water to produce an aqueous base soluble carboxylic acid (Figure 1). However, unlike DNQ, the photoproducts of DC exhibited transparency in the 240–260-nm range.

The reactivity of the ketene intermediate also has a strong influence on the utility of the compound in the photolithographic process. For maximum efficiency the ketene intermediate must be highly selective and react rapidly but exclusively with water to form the carboxylic acid rather than with the phenolic resin to form an ester. To the extent that the ketene reacts with the resin, a lower solubility rate is produced, leading to lower imaging contrast and poor performance of the resist formulation.[13,14] Stabilization of the ketene intermediate should make it less reactive and therefore more selective toward hydration. To that end, a study of substituent effects on the reaction kinetics of the diazocoumarin-derived ketenes has been conducted and is presented here.

Experimental Section

Characterization. ^{1}H and ^{13}C NMR spectra were recorded on a GE-300 spectrometer. Chemical shifts were internally referenced to the residual proton signals of the solvents shown. Thermal gravimetric analysis (TGA) and differential scanning calorimetry (DSC) were performed at a scan rate of 10 °C/min. Mass spectra (MS) were obtained using either fast atom bombardment (FAB) ionization or chemical ionization (CI). All
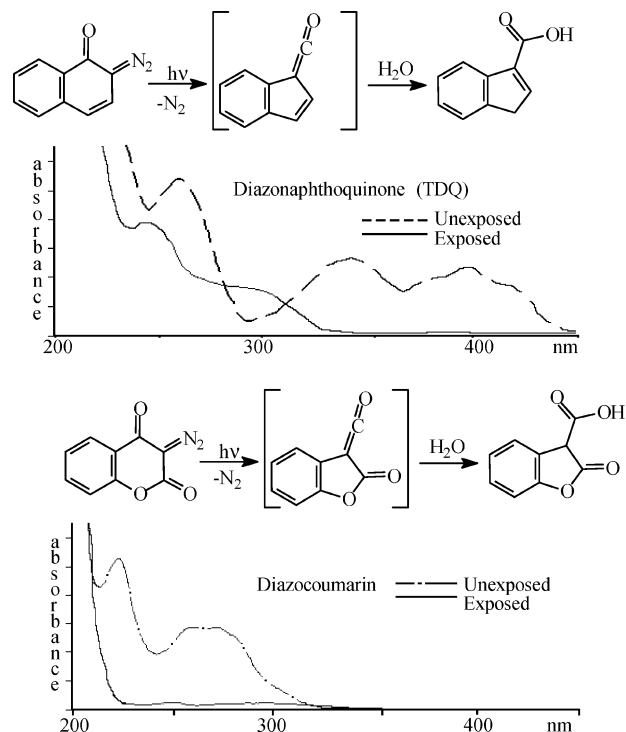

Figure 1. Absorption spectra of a diazonaphthoquinone and a 3-diazo-4-oxocoumarin in acetonitrile solution. Note the similarity in the photochemical reactions and the important difference in the spectral characteristics. The diazocoumarin bleaches after exposure to DUV while the diazonaphthoquinone does not (absorbance normalized and measured in arbitrary units).

reactions were carried out under an N_2 atmosphere unless otherwise stated.

Solvents and Reagents. Tetrahydrofuran (THF) was distilled from sodium and benzophenone. Triethylamine was distilled from KOH and stored over molecular sieves. All other reagents were purchased and used as received. Tosyl azide was synthesized according to published procedures[15] and should be used with caution.[24]

General Procedure for the Selectively Protected Dihydroxycoumarin Compounds: 1ih–1j. A solution of the dihydroxycoumarin was dissolved in dry THF in a round-bottomed flask. To this solution was added an excess (at least 10-fold) of triethylamine and the resulting mixture was stirred for 10 min. A solution of 1 equiv of the required chloride in dry THF (~1 M) was added dropwise to the flask and the resulting mixture was stirred at room temperature overnight. Enough acetone was added to double the reaction volume and the precipitated salts were filtered out. The filtrate was concentrated by rotary evaporation and the residue was dried under vacuum to give the title product. This was used without purification in the diazotization step.

4-Hydroxy-7-methanesulfonyloxycoumarin (1h). Prepared from reaction of 4,7-dihydroxycoumarin with methane sulfonyl chloride. Yield: 70.6%. ^{1}H NMR (DMSO-d_6): δ 3.37 (3 H, s), 5.01 (1 H, s), 7.19 (1 H, dd, J = 8.5, 1.9 Hz), 7.27 (1 H, d, J = 1.9 Hz), 7.95 (1 H, d, J = 8.5 Hz). ^{13}C NMR (DMSO-d_6): δ 37.6, 87.8, 110.0, 117.0, 119.3, 125.6, 150.8, 154.7, 163.4, 170.7. MS (CI): m/z (rel. intensity) 257 (M$^+$ + 1, 100), 256 (7), 179 (48), 130 (9). HRMS (FAB): m/z calcd for $C_{10}H_9O_6S$ (M + H$^+$) 257.0120, found 257.0121.

4-Hydroxy-7-methoxycarbonyloxycoumarin (1i). Prepared from reaction of 4,7-dihydroxycoumarin with methoxy-carbonic chloride. Yield: 71.9%. ^{1}H NMR (DMSO-d_6): δ 3.85 (3 H, s), 4.82 (1 H, s), 7.03 (1 H, dd, J = 8.6, 1.9 Hz), 7.09 (1

(8) Aviram, A.; Angelopoulos, M.; Babich, E. D.; Babich, I. V.; Petrillo, K.; Seeger, D. E. *Proc. SPIE's 23rd Annu. Int. Symp. Microlithogr.* **1998**, *3331*, 349.

(9) Reichmanis, E.; Wilkins, C. W., Jr.; Chandross, E. A. *J. Vac. Sci. Technol.* **1981**, *ED-28* (11), 1300.

(10) Hayase, S.; Horiguchi, R.; Onishi, K.; Gokochi, T. *Jpn. Kokai Tokkyo Koho* Patent. JP 02061640 A2 900301 *Heisei*, JP 88-211835 880826, 1990, 1.

(11) (a) Meier, H.; Zeller, K. P. *Angew. Chem., Int. Ed.* **1975**, *14*, 32. (b) Kaplan, F.; Meloy, G. K. *J. Am. Chem. Soc.* **1966**, *88* (5), 950. (c) Tomioka, H.; Hayashi, N.; Tsuneo, A.; Izawa, Y. *Bull. Chem. Soc. Jpn.* **1983**, *56*, 758. (d) Willson, C. G. *Introduction to Microlithography 2d*; American Chemical Society: Washington, DC, 1994; pp 162–170. (e) Tidwell, T. T. *Ketenes*; John Wiley & Sons: New York, 1996.

(12) Pacansky, J.; Lyerla, J. R. *IBM J. Res. Dev.* **1979**, *23* (1), 42.

(13) Grant, B. D.; Clecak, N. J.; Twieg, R. J.; Willson, C. G. *IEEE Trans. Electron Devices* **1981**, *28* (11), 1300.

(14) Willson, C. G.; Miller, R. D.; McKean, D. R.; Pederson, L. A.; Regitz, M. *SPIE vol. 771 Adv. Resist Technol. Process. IV* **1987**, 2.

(15) Previously reported, but not characterized, by Lee, Y. R.; Suk, J. Y.; Kim, B. S. *Tetrahedron Lett.* **1999**, *40*, 6603.

H, d, $J = 1.9$ Hz), 7.84 (1 H, d, $J = 8.5$ Hz). ^{13}C NMR (DMSO-d_6): δ 55.6, 86.3, 108.8, 115.4, 120.0, 125.2, 152.2, 153.3, 155.1, 164.1, 173.5. MS (CI): *m/z* (rel. intensity) 237 (M[+] + 1, 100), 236 (6), 221 (22), 179 (5), 102 (43), 101 (46), 100 (39). HRMS (FAB): *m/z* calcd for $C_{11}H_9N_2O_6$ (M + H^{+}) 237.0399, found 237.0399.

5-*tert*-Butyldimethylsilyl-4-hydroxycoumarin (1j). In deviation from the general procedure: One gram of 4,5-dihydroxycoumarin was added to 10 mL of benzene. To this was slowly added 0.855 g (1.01 equiv) of *tert*-butyldimethylsilyl chloride and 20 mL of triethylamine. The reaction was then refluxed for 5 h, cooled, filtered, and rotary-evaporated to remove the benzene and excess triethylamine. The resulting product was analyzed by NMR and MS, which verified the material was sufficiently pure for the diazotization reaction. Yield: 99%. ^{1}H NMR (DMSO-d_6): δ 0.01 (6 H, s), 0.95 (9 H, s), 4.75 (1 H, s), 6.40 (1 H, d, $J = 8.5$ Hz), 6.49 (1H, dd, $J_1 = 8.2$, $J_2 = 1.9$ Hz), 7.17 (1 H, t, $J = 8.2$ Hz). MS (EI): *m/z* (rel intensity) 293 (M + H^{+}, 100), 231 (10), 205 (20), 179 (45). HRMS (EI): *m/z* calcd for $C_{15}H_{20}O_4Si$ (M + H^{+}) 292.1209, found 292.1216.

General Procedure for 3-Diazo-4-oxocoumarin Compounds 2a−e and 2i−k. A solution of the appropriate 4-hydroxycoumarin in dry THF was placed in a round-bottomed flask and cooled to −20 °C (2-propanol/dry ice bath). To this solution was slowly added 1 equiv of triethylamine. The resulting mixture was stirred for 10 min. To it a solution of 1.1 equiv of *p*-toluenesulfonyl azide[24] in dry THF was added dropwise. The reaction mixture was stirred at −20 to −15 °C for 2 h. It was then allowed to warm to room temperature and then decanted and the solvent was removed by rotary evaporation. The residue was purified by column chromatography (silica gel, hexane/ethyl acetate = 1/1) and recrystallized from methanol to give the title product in the yield shown.

3-Diazo-4-oxocoumarin (2a). Yield 74%. FT-IR (KBr): ν_{max} 1347, 1460, 1611, 1642, 1723 (d), 2177, 2202 cm^{−1}. ^{1}H NMR (DMSO-d_6): δ 7.30 (1 H, d, $J = 8.2$ Hz), 7.36 (1 H, t, $J = 7.3$ Hz), 7.68 (1 H, td, $J = 7.8$, 1.8 Hz), 8.05 (1 H, dd, $J = 7.9$, 1.6 Hz). ^{13}C NMR (DMSO-d_6): δ 115.31, 117.87, 118.90, 125.20, 125.79, 136.07, 153.70, 157.94, 173.92. MS (CI): *m/z* (rel. intensity) 189 (M[+] + 1, 100). Anal. Calcd for $C_9H_4N_2O_3$: C, 57.46; H, 2.14. Found: C, 57.47; H, 2.18. TGA onset of decomposition 166 °C. DSC: melting point 158 °C, $\Delta H = 140.68$ J/g.

3-Diazo-7-methyl-4-oxocoumarin (2b).[15] Yield 22%. FT-IR (KBr): ν_{max} 2923, 2177, 1737 (d), 1656, 1622, 1336, 1321 cm^{−1}. ^{1}H NMR (DMSO-d_6): δ 2.42 (3 H, s), 7.26 (2 H, m), 7.82 (1 H, d, $J = 8.1$ Hz). ^{13}C NMR (DMSO-d_6): δ 21.3, 116.4, 117.8, 124.8, 126.3, 147.7, 153.4, 153.6, 158.0, 173.6. MS (CI): *m/z* (rel. intensity) 203 (M[+] + 1, 100), 175 (56), 135 (13), 118 (12). Anal. Calcd for $C_{10}H_6N_2O_3$: C, 59.41; H, 2.99. Found: C, 58.78; H, 2.93. TGA onset of decomposition 178 °C. DSC: melting peak 177.1 °C, $\Delta H = 105.7$ J/g.

3-Diazo-7-methoxy-4-oxocoumarin (2c). Yield 34% of light orange crystals. FT-IR (KBr): ν_{max} 1311, 1438, 1611, 1667, 1729 (d), 2177 (d), 2930 cm^{−1}. ^{1}H NMR (acetone-d_6): δ 3.85 (3 H, s), 5.94 (1 H, s), 6.02 (1 H, d), 7.73 (1 H, d). ^{13}C NMR (DMSO-d_6): δ 55.4, 110.8, 115.6, 118.0, 129.7, 149.9, 153.9, 154.0, 163.2, 178.5. MS (CI): *m/z* (rel. intensity) 219 (M[+] + 1, 100), 191 (80), 163 (62), 151 (31), 134 (30). Anal. Calcd for $C_{10}H_6O_4N_2$: C, 55.05; H, 2.77. Found: C, 55.1; H, 2.8. TGA onset of decomposition 192 °C. DSC: melting peak 184 °C, $\Delta H = 86.7$ J/g.

5-Benzyloxy-3-diazo-4-oxocoumarin (2d). Yield 20%. FT-IR (KBr): ν_{max} 2168, 1724, 1659, 1604, 1454, 1319, 1100 cm^{−1}. ^{1}H NMR (DMSO-d_6): δ 5.14 (2 H, s), 7.4−7.5 (8 H, m). ^{13}C NMR (DMSO-d_6): δ 64.9, 96.3, 109.2, 113.1, 127.7, 128.4, 136.6, 139.3, 153.7, 155.3, 164.8, 181.1. MS (CI): *m/z* (rel. intensity) 295 (M[+] + 1, 100), 267 (20), 238 (13), 181 (66), 131 (12), 119 (9). Anal. Calcd for $C_{16}H_{10}N_2O_4$: C, 65.31; H, 3.43. Found: C, 64.35; H, 3.70. TGA onset of decomposition 170 °C. DSC: melting peak 156.0 °C, $\Delta H = 107.1$ J/g.

6-Benzyloxy-3-diazo-4-oxocoumarin (2e). Yield 22%. FT-IR (KBr): ν_{max} 1324, 1444, 1489, 1644, 1729 (d), 2173 cm^{−1}. ^{1}H NMR (DMSO-d_6): δ 5.40 (2 H, s), 7.21 (2 H, m), 7.34 (5 H,

m), 7.77 (1 H, d, $J = 8.36$ Hz). ^{13}C NMR (DMSO-d_6): δ 89.6, 103.8, 107.2, 110.7, 132.8, 154.6, 155.7, 161.7, 167.9. MS (CI): *m/z* (rel. intensity) 295 (M[+] + 1, 100), 267 (12), 217 (6). Anal. Calcd for $C_{16}H_{10}N_2O_4$: C, 65.31; H, 3.43. Found: C, 65.58; H, 3.54. TGA onset of decomposition 153.7 °C. DSC: melting peak 209 °C, $\Delta H = 186.9$ J/g.

3-Diazo-7-methanesulfonyloxy-4-oxocoumarin (2h). Yield 46%. FT-IR (KBr): ν_{max} 3031.4, 2194.1, 1732.4, 1655.4, 1614.7, 1447.2, 1383.9, 1347.7, 1329.6, 1184.7, 1134.9 cm^{−1}. ^{1}H NMR (DMSO-d_6): δ 3.53 (3 H, s), 7.42 (1 H, dd, $J = 8.6$, 1.9 Hz), 7.52 (1 H, d, $J = 1.9$ Hz), 8.05 (1 H, d, $J = 8.5$ Hz). ^{13}C NMR (DMSO-d_6): δ 38.0, 111.8, 117.7, 119.3, 127.2, 153.8, 154.1, 154.2, 157.5, 172.9. MS (CI): *m/z* (rel. intensity) 283 (M[+] + 1, 100), 282 (20), 257 (4), 255 (34), 215 (4), 177 (4), 175 (5). MS (FAB): *m/z* calcd for $C_{10}H_7N_2O_6S$ (M + H^{+}) 283.0020, found 283.0025. Anal. Calcd for $C_{10}H_6N_2O_6$: C, 42.56; H, 2.14; N, 9.93; S, 11.36. Found: C, 42.58; H, 2.20; N, 9.84; S, 11.25. mp 140−142 °C. TGA onset of decomposition 192.5 °C. DSC: peak 133.8 °C and 141.2 °C, onset 204.2 °C.

3-Diazo-7-methoxycarbonyloxy-4-oxocoumarin (2i). Yield 42%. FT-IR (KBr): ν_{max} 2189.5, 1786.7, 1732.4, 1655.4, 1623.8, 1438.2, 1325.0, 1248.1 cm^{−1}. ^{1}H NMR (DMSO-d_6): δ 3.88 (3 H, s), 7.36 (1 H, dd, $J = 8.6$, 1.9 Hz), 7.47 (1 H, d, $J = 1.9$ Hz), 8.02 (1 H, d, $J = 8.5$ Hz). ^{13}C NMR (DMSO-d_6): δ 56.0, 111.0, 116.9, 118.7, 126.7, 152.6, 154.0, 154.1, 155.9, 157.7, 173.1. MS (CI): *m/z* (rel. intensity) 263 (M[+] + 1, 100), 262 (33), 235 (17), 195 (3), 154 (2), 134 (9), 106 (4). MS (FAB): *m/z* calcd for $C_{11}H_7N_2O_6$ (M + H^{+}) 263.0304, found 263.0307. Anal. Calcd for $C_{11}H_6N_2O_6$: C, 50.39; H, 2.31; N, 10.68. Found: C, 50.62; H, 2.37; N, 10.61. mp 168−170 °C. TGA onset of decomposition 204.6 °C. DSC: peak 177.7 °C, onset 211.4 °C.

3-Diazo-4-oxo-5-*tert*-butyldimethylsilylcoumarin (2j). Yield 41%. FT-IR (KBr): ν_{max} 2189.5, 1786.7, 1732.4, 1655.4, 1623.8, 1438.2, 1325.0, 1248.1 cm^{−1}. ^{1}H NMR (DMSO-d_6): δ 0.73 (6 H, s), 1.30 (9 H, s), 7.21 (2 H, t, $J = 9.1$ Hz), 7.98 (1 H, t, $J = 8.4$ Hz). ^{13}C NMR (DMSO-d_6): δ −3.2, 21.1, 26.8, 61.4, 89.0, 94.6, 108.3, 118.4, 158.8, 162.4, 171.7, 177.3. MS (CI): *m/z* = 319 (M[+]). Anal. Calcd for $C_{15}H_{18}N_2O_4Si$: C, 56.58; H, 5.70. Found: C, 56.34; H, 5.47.

Procedure for Kinetic Studies of Ketene Reactivity Using FT-IR. The semiempirical calculations were performed using the AM1-SM2 basis set and the default geometry minimization settings.[31]

The diazocoumarins were formulated in a standard novolac polymer solution at 0.532 *m* for the kinetic measurements. Photoresists are typically formulated by "weight percent" PAC. The samples for this investigation were formulated to give a constant molality.

The samples were spin-coated onto polished sodium chloride disks 5 mm in diameter and 2-mm thick. These samples were then baked on a 90 °C hot plate for 2 min to remove the casting solvent. Samples were also coated onto silicon wafers under the same conditions and their coating thickness (1.2−2.2 μm) was determined using a profilometer. The coated samples were stored in a vacuum desiccator wrapped in aluminum foil until needed for the kinetics experiment. The samples were then introduced into a modified cryostat operated inside a FT-IR spectrometer, with an exposure tool using a 500-W mercury arc lamp and power supply attached as shown in Figure 2. After all the parts were assembled and a basic experimental protocol was established, some data was taken to test the instrument for reproducibility. The temperature controller was replaced with a copper thermocouple using the appropriate adhesive to the sample holder of the cryostat. Introduction of the thermocouple was completed by rewiring the data cable of the temperature controller to accommodate an outside thermocouple. It was necessary to change the dip switch settings on the board inside the controller and then calibrate the sensor. The proportional, integral, and derivative control parameters were also changed to account for the long response time of the system, which necessitated the installation of the new sensor.

Samples were introduced into the cryostat at room temperature and the sample compartment was pumped out and back-
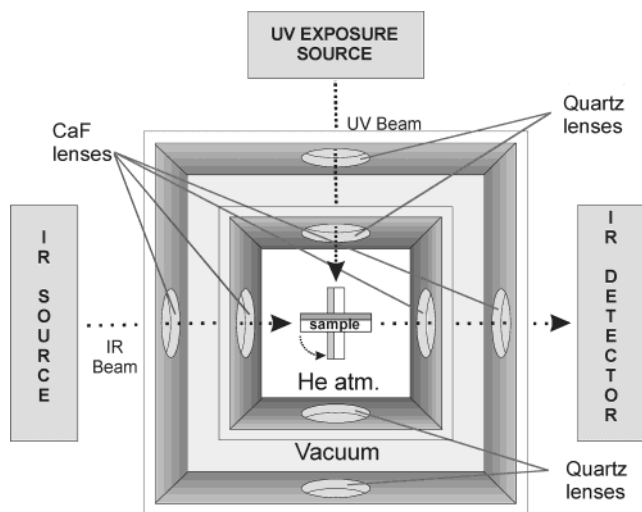
Figure 2. A schematic diagram of the instrumentation used for the kinetic measurements.

filled with helium several times. The sample compartment was then evacuated (20–80 mTorr) and the sample was warmed to between 40 and 60 °C for between 2 and 5 h. The liquid nitrogen coolant reservoir of the cryostat was filled, the sample chamber was back-filled again with helium, and the sample was cooled. The experiments were run at atmospheric pressure and 200 K. Careful adjustment of the nitrogen flow rate was necessary to maintain the desired temperature. The sample temperature was allowed to stabilize, which typically took between 30 and 90 min. The sample was scanned by the IR spectrometer and rotated into the path of the UV exposure tool, the shutter was actuated to expose the sample, and it was rotated back into the IR beam path. Exposures were done using the full spectrum of the lamp to minimize exposure times that were 2 min for the diazocoumarins and 20 s for the DNQ (TDQ).

The FT-IR spectra were collected using eight scans each with a resolution of four reciprocal centimeters at regular intervals. Because the exact position of the ketene peak shifted as a function of the substrate, the boundaries of the baseline and area to be integrated were chosen separately for each compound tested. The peak area data was correlated with the time stamp for each spectrum using the first spectra as time equals zero. The rate constants described in the Results and Discussion section represent the average of between three and six measurements for each substrate discussed with a standard deviation of 0.021 (8%).

Results and Discussion

Synthesis. The substituted 3-diazo-4-oxocoumarins used in this study were prepared by diazotization of the corresponding substituted 4-hydroxycoumarin. A variety of 4-hydroxycoumarin derivatives were investigated for this study and were prepared by adaptations of previously reported procedures (Schemes 2 and 3).

The 7-methyl analogue **1b** was made by Friedel–Crafts like cyclization of bis-3-hydroxyphenyl-malonate using aluminum chloride, a reaction based on the work of Ziegler and Junek.[16] 7-Methoxy-4-hydroxycoumarin **1c** was prepared via the cyclization reaction between 4-methoxyacetophenone and diethyl carbonate.[17] The route to 5- and 6-benzoxycoumarin compounds **1d** and **1e** involved the Claisen-like condensation and cyclization of diethyl carbonate with 2-hydroxyacetophenone

Scheme 2. Diazotization of Functionalized 4-Hydroxycoumarins
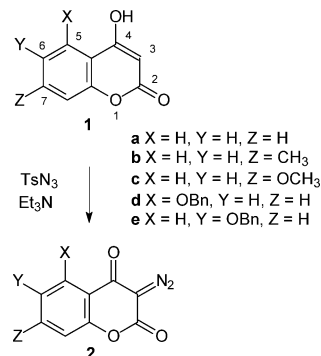
Scheme 3. Substitution and Diazotization of Phenolic 4-Hydroxycoumarins
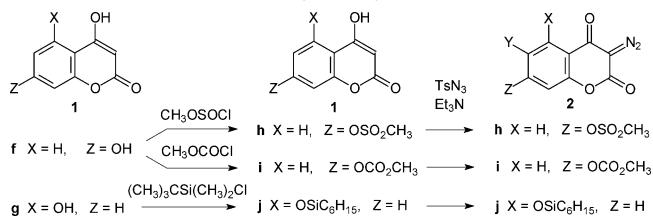
bearing benzyoxy groups in either the 5- or 6- positions, respectively.[18,19]

Preparation of the protected alcohols, **1h–j**, involved selective protection of the 5- or 7-hydroxy groups of **1f** or **1g** (Scheme 3). The 4,7-dihydroxycoumarin **1f** had been prepared by the reaction of cyanoacetic acid with resorcinol published by Sonn,[20] to produce the 4-amino-coumarin (ketimine) which could be hydrolyzed in acid to provide the dihydroxycoumarin. Although Sonn (in 1917) reported the isolation of the ketimine before the hydroylsis step, our characterization was more consistent with an enamine. The synthesis of the 4,5-dihydroxycoumarin, **1g**, utilized a high-temperature cyclization of resorcinol with diethyl malonate.[21,22] The phenolic 5- or 7-positions of **1f** and **1g** could be protected using standard etherification or esterification procedures, but selectivity over the 4-position was only achieved at low temperatures (−20 °C).

Diazotization. The photoactive compounds **2a–e** and **2h–j** were prepared by diazotization of the substituted 4-hydroxycoumarins, **1a–e** and **1h–j**. This transformation was carried out using tosyl azide[23] following previously reported procedures.[24,25]

Materials Properties. The 3-diazo-4-oxocoumarins are typically white, crystalline materials that are stable at room temperature in air and do not exhibit the high shock sensitivity that has been observed in some other diazo compounds.[26] These materials have been investigated using both thermal gravimetric analysis (TGA)

(16) Ziegler, E.; Junek, H. *Monatsh. Chem.* **1955**, *86*, 29.
(17) Boyd, J.; Robertson, A. *J. Chem. Soc.* **1948**, 174.

(18) Hermodson, M. A.; Barker, W. M.; Link, K. P. *J. Med. Chem.* **1967**, *14* (2), 167.
(19) Dickenson, H. G.; Ward, Blenkinsop and Co., Ltd., U.S. Patent 2,449,162, Sept 14, 1948 [*Chem. Abstr.* **1949**, *43*, 694].
(20) Sonn, A. *Ber.* **1917**, *50*, 1292.
(21) Castleberry, B.; Valente, E. J.; Eggleston, D. S. *J. Cryst. Spec. Res.* **1990**, *20* (6), 583.
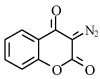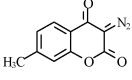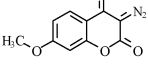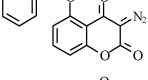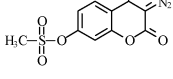(22) Trivedi, R. N. *Curr. Sci. (India)* **1961**, *30*, 54.
(23) Regitz, M.; Hocker, J.; Liedhegener, A. *Org. Synth. Collect.* **1973**, *5*, 179.
(24) Regitz, M. *Angew. Chem., Int. Ed.* **1967**, *6*, 9, 733.
(25) Hendrickson, J. B.; Wolf, W. A. *J. Org. Chem.* **1968**, *33*, 9, 3610.

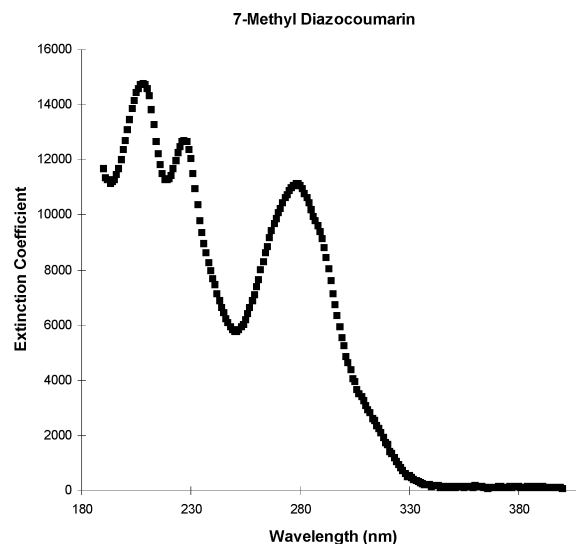|	T_m °C	ε_{248}	T_d °C
	157	7,000	166
	177	6,000	178
	183	10,000	191
	156	3,000	170
	140	8,000	192

Figure 3. A representative sample of substituted diazocoumarins. T_m is the melting point and T_d is the decomposition temperature. The extinction coefficients (ε_{248}) were measured at 248 nm in acetonitrile solution. The inset picture shows the extinction coefficient (M^{-1} cm^{-1}) as a function of wavelength (nm) of the 7-methyl derivative.

and differential scanning calorimetry (DSC). The melting points and decomposition temperatures of many of the derivatives nearly overlap and are summarized in Figure 3. Of particular interest, many of these compounds are stable at 150 °C unlike DNQ, allowing higher baking temperatures and longer baking times, both of which contribute to improved adhesion and contrast.[27] The extinction coefficient at 248 nm of the analogues studied varies by a factor of approximately 3. This large variance is a caused by a narrow local minimum in the absorbance spectra near 248 nm (Figure 3) As a result, small shifts in the absorbance spectrum due to substituent effects cause large changes in the absorbance at 248 nm. The quantum efficiencies of these compounds were measured by calculating the disappearance of the starting material, as determined by the change in the absorbance. The quantum efficiencies varied from 0.3 to 0.4, similar to the corresponding diazonaphthoquinones. Overall, the physical properties of these photoactive compounds are comparable to DNQ, and therefore are appropriate for applications in microlithography.

Kinetics. One of the key characteristics in determining the utility of a ketene PAC is its selectivity in reacting with water, to form a soluble carboxylic acid, rather than with the phenolic resin, which would reduce the solubility of the exposed resist. Therefore, it is useful to identify which structural variations of the ketene PAC react most selectively with water. However, in order for the study to produce meaningful results for lithographic application, the experiments must be carried out in a thin film, rather than in solution. Because it would be prohibitively complicated to accurately measure and maintain an exact concentration of water in the film, the study was designed to measure reactivity
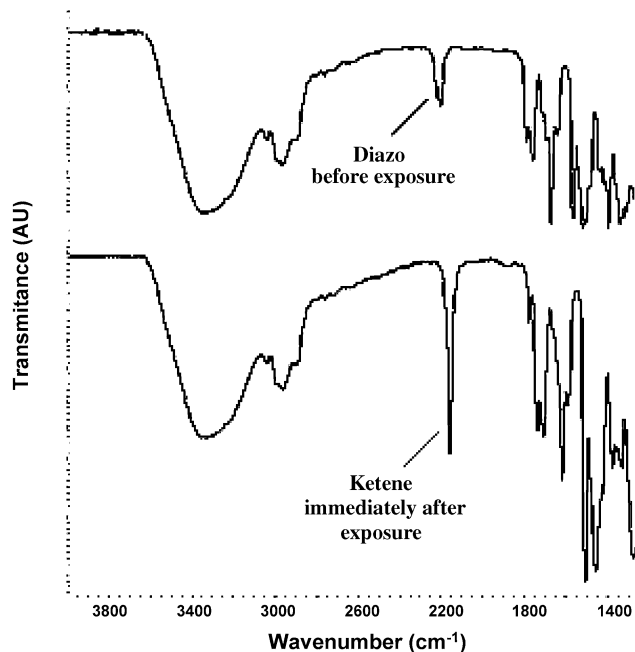
(26) Regitz, M.; Hocker, J.; Liedhegener, A. *Org. Synth. Collect.* **1973**, *5*, 179 notes the explosive nature of diazo compounds. Striking a sample of 3-diazo-4-oxocoumarin with a hammer on a steel plate with much more force than is required to detonate the diazonaphthoquinone TDQ did not result in any observable detonation.

(27) Mack, C. A.; Mueller, K. E.; Gardiner, A. B.; Qiu, A.; Dammel, R. R.; Koros, W. G.; Willson, C. G. *Proc. SPIE: Int. Soc. Opt. Eng. 3049*, **1997**, 355.
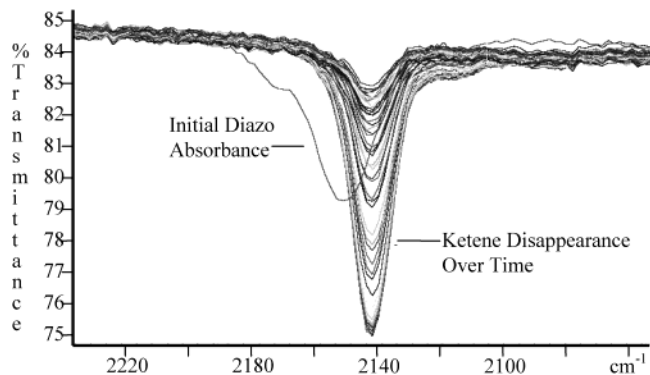

Figure 4. Infrared spectra of a dry resist film at 200 K before and after exposure.

instead with a novolac film in anhydrous conditions. Because the reaction with water is greatly favored, those that react most slowly with the anhydrous novolac resin are least reactive, and therefore would be expected to be most selective toward reaction with water. An optical cryostat was constructed that allows resist films to be exposed to UV radiation and to be observed using an FT-IR detector while strictly controlling the temperature, pressure, and atmosphere in the reaction chamber. The experiments were conducted by spin coating a film consisting of 0.5 M PAC in novolac resin on a NaCl substrate, exposing the sample to vacuum at slightly elevated temperature to remove any water and then back-filling the apparatus with a dry inert gas (He). The sample was then cooled to 200 K and exposed to 240−260-nm radiation through a quartz window, which generated the ketene (Figure 4).[26,27] When the exposure

Figure 5. The change in absorbance as a function of time.
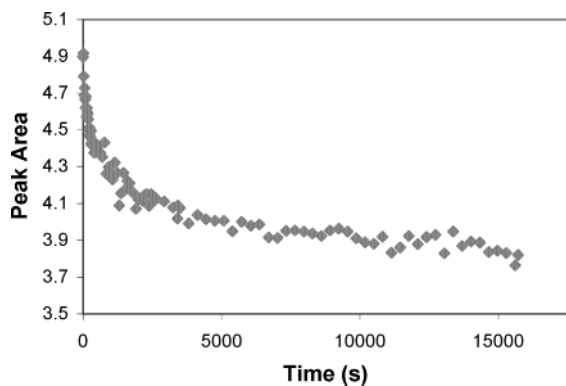
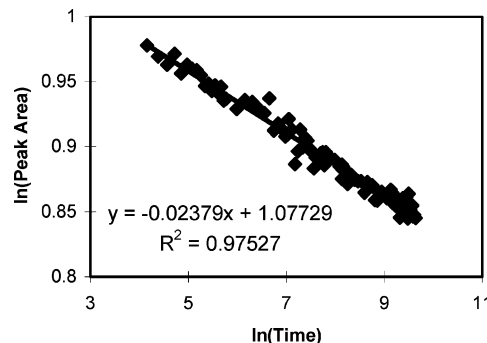**Figure 6.** An example of the raw kinetic data for the absorbance of 7-methyl diazocoumarin.

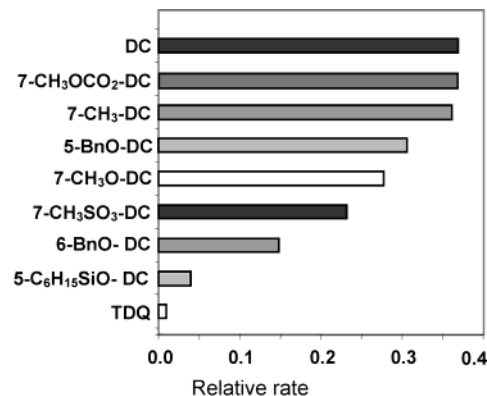**Figure 7.** The normalized log of absorbance vs log of time for 7-methyl diazocoumarin.
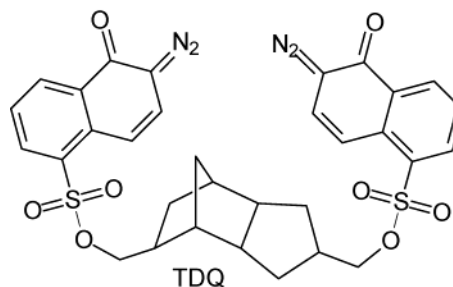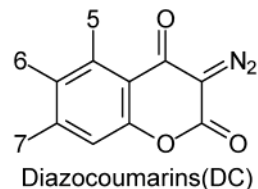
Figure 8. Rate constants for ketenes generated by the substrates shown.

was complete, the sample was rotated into the IR beam and the temperature was quickly adjusted to the desired set point. Measuring the attenuation of the ketene IR absorbance allowed quantification of the extent of reaction between the ketene and the resin as a function of time (Figure 5).

The ketenes obtained under these controlled conditions were sufficiently stable to exhibit clear trends in structure reactivity relationships. The relative concentration of ketene at any time was calculated by integrating the area of the ketene absorbance peak. The rate of reaction could be examined by plotting the relative concentration against time (Figure 6). Because these reactions took place in a film, they could not be analyzed by standard solution phase kinetics. One method previously used to analyze the kinetics of reactions in a polymer film involved breaking the data into two distinct regimes, one describing the initial fast rate and the second describing the slower rate of the long-term reaction.[6,28] This approach seemed much too subjective in this particular case because it was difficult to determine the transition point between these two separate regimes, without incorporating human bias. So an alternative model for describing the kinetics of this system was sought.

Kinetic studies in polymer systems have previously[29] been modeled using fractal mathematics. The concept of "fractal time" has proven to be very useful for explaining the temporal scaling laws of many phenomena involving condensed matter.[30] The observation that the current system seems to obey such a scaling law is consistent with the fact that these reactions are taking place in a polymer glass rather than in solution. In accordance with this model, the absorbance peak area was plotted against log time, to yield a straight line (Figure 7). The slope of the best fit line was then used as a relative rate constant, to quantitatively compare the reactivity of the different coumarins. The correlated rate constants for the different substrates are shown in Figure 8.

(28) (a) Leeson, M. J.; Willson, C. G.; Pawloski, A.; Yueh, W.; Levering, V. *Proc. SPIE: Int. Soc. Opt. Eng. 3049*, **1997**, 861. (b) Willson, C. G.; Leeson, M. J.; Yeuh, W.; Steinhausler, T.; McAdams, C. L.; Levering, V.; Pawloski, A.; Aslam, M.; Vicari, R.; Sheehan, M. T.; Sounik, J. R.; Dammel, R. R. *Proc. SPIE: Int. Soc. Opt. Eng. 3049*, **1997**, 226. (c) Leeson, M. J.; Willson, C. G.; Steinhausler, T.; Yueh, W. *Techcon 1996 Conf. Semicond. Res. Corp.* **1996**.

(29) (a) Chow, T. S. *Macromolecules* **1992**, *25*, 440. (b) Dewey, T. G. *J. Chem. Phys.* **1990**, *92, 12*, 7426. (c) Byers, B. D.; Friedrichs, M. S.; Friesner, R. A.; Webber, S. E. *Macromolecules* **1988**, *21*, 3402.
(30) Schlesinger, M. F. *Annu. Rev. Phys. Chem.* **1988**, *39*, 269.
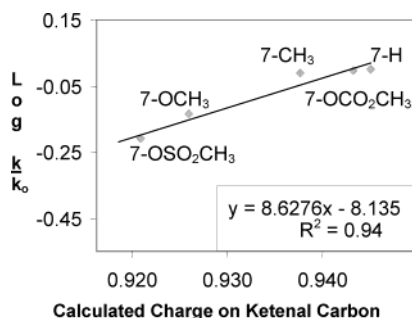
Figure 9. Rate constant correlation to charge for all of the diazocoumarins substituted in the 7-position (see Figure 8 for structures).
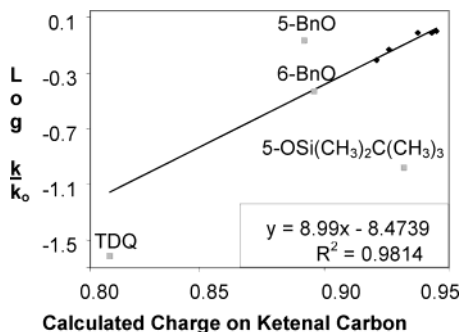

Figure 10. Rate constant vs charge data for all of the compounds shown in Figure 8.

During comparison of the relative rates, it was discovered that the majority of the compounds exhibited a Hammett-like trend, where the reactivity rates corresponded directly to the substituents ability to electronically stabilize the ketene intermediate. Instead of applying the traditional Hammett values, some of which were unavailable for the substituents used, molecular modeling was used to calculate the partial charge carried on the ketene carbon as a result of substituent effects.

Charge to Rate Correlation. The charge at the ketenyl carbon was calculated using the Spartan molecular modeling software package.[31] The charge on this atom was chosen for comparison because it should correlate to the reactivity of the ketene toward nucleophilic attack. Previous studies of this reaction have concluded that the nucleophilic attack on this carbon is the rate-determining step.[32] When the calculated charge is plotted against the relative rate constants for each ketene derivative, a linear trend is observed for ketenes with substituents on the 7-positions (Figure 9) as well as the 6-position (Figure 10). This trend fits the theoretical prediction that reduction of the partial positive charge on the ketenyl carbon by inductive donation of electron density reduces the ketenes reactivity, and hence a slower reaction rate is observed.

The linear trend is not observed with the substituents in the 5-position (Figure 10), but because of the proxim-

ity of the 5-position to the reactive center, it was expected to be more susceptible to secondary effects, such as steric effects. For example, the bulky 5-*tert*-butyldimethylsiloxy group exhibits a rate significantly lower than predicted by purely electronic considerations, but such a large group adjacent to the ketene is expected to hinder access to the reactive site. A more surprising result is the enhanced rate of the 5-benzyloxy derivative over the predicted rate. Some additional favorable interaction, between the benzyl substituent and the phenolic polymer, must be responsible for the faster rate. Additional studies with a wider variety of substituents should elucidate the nature of these secondary effects.

Conclusions

3-Diazo-4-oxocoumarins exhibit the spectral, photochemical, and thermal properties required for use in the design of PACs for nonchemically amplified DUV resists. A kinetic study of the reaction of the ketene intermediate showed that it is possible to tailor the reactivity of this key intermediate by modification of the substituents on the aromatic ring. The reactivity of the ketenes with substituents in the 6- and 7-positions corresponds closely to the calculated charge on the ketenyl carbon. Substituents capable of electron donation inductively or through resonance yielded the most stable and therefore most selective ketenes. This information should prove valuable in optimizing the design of photoactive compounds for use in future microlithographic systems.

It should be noted that while these diazoketones are relatively thermally stable, their rearrangement products are β-keto acids that are susceptible to decarboxylation at elevated temperatures, limiting the use of the traditional postexposure bake during positive tone development. However, this decarboxylation can be exploited to invert the tone of the resist action, allowing the resist to be printed in negative tone.[1] After initial exposure and bake, the unexposed polymer can be stripped by flood exposure and dissolution of the resultant carboxylate resin with aqueous base, leaving the negative tone image of the decarboxylated resin behind. This is a useful process, analogous to that which occurs upon the addition of bases to the diazonaphthoquinone−novolac system.[33]

(31) PC Spartan Version 1.1, Wavefunction Inc., Irvine, CA, 1996.
(32) Tidwell, T. T. *Ketenes*; John Wiley & Sons: New York, 1995.

(33) MacDonald, S. A.; Miller, R. D.; Willson, C. G.; Feinberg, G. M.; Gleason, R. T.; Halverson, R. M.; MacIntyre, M. W.; Motsiff, M. T. *Kodak Microelectron. Sem.* **1982**, *23*, 114.